1-1-2014

Absolute phase map recovery of two fringe patterns with flexible selection of fringe wavelengths

Jiale Long
Huazhong University of Science and Technology

Jiangtao Xi
University of Wollongong, jiangtao@uow.edu.au

Ming Zhu
Huazhong University of Science and Technology

Wenqing Cheng
Huazhong University of Science and Technology

Rui Cheng
Huazhong University of Science and Technology

See next page for additional authors

Absolute phase map recovery of two fringe patterns with flexible selection of fringe wavelengths

Abstract

A novel approach is proposed to unwrap the phase maps of two fringe patterns in fringe pattern projection-based profilometry. In contrast to existing techniques, where spatial frequencies (i.e., the number of fringes on a pattern) of the two fringe patterns must be integers and coprime, the proposed method is applicable for any two fringe patterns with different fringe wavelengths (i.e., the number of pixels in a fringe) and thus provides more flexibility in the use of fringe patterns. Moreover, compared to the existing techniques, the proposed method is simpler in its implementation and has better antierror capability. Theoretical analysis and experiment results are presented to confirm the effectiveness of the proposed method.

Keywords

absolute, phase, wavelengths, map, selection, recovery, flexible, patterns, fringe, two

Disciplines

Engineering | Science and Technology Studies

Publication Details

Long, J., Xi, J., Zhu, M., Cheng, W., Cheng, R., Li, Z. & Shi, Y. (2014). Absolute phase map recovery of two fringe patterns with flexible selection of fringe wavelengths. Applied Optics, 53 (9), 1794-1801.

Authors

Jiale Long, Jiangtao Xi, Ming Zhu, Wenqing Cheng, Rui Cheng, Zhongwei Li, and Yusheng Shi

Absolute phase map recovery of two fringe patterns with flexible selection of fringe wavelengths

Jiale Long,[1,4] Jiangtao Xi,[2,*] Ming Zhu,[1] Wenqing Cheng,[1] Rui Cheng,[1] Zhongwei Li,[3] and Yusheng Shi[3]

[1]Department of Electronic and Information Engineering, Huazhong University of Science and Technology, Wuhan, Hubei 430074, China

[2]School of Electrical Computer and Telecommunications Engineering, University of Wollongong, Wollongong, NSW 2522, Australia

[3]State Key Laboratory of Material Processing and Die & Mould Technology, Huazhong University of Science and Technology, Wuhan, Hubei 430074, China

[4]School of Information, Wuyi University, Jiangmen, Guangdong 529020, China

*Corresponding author: jiangtao@uow.edu.au

Received 3 December 2013; revised 5 February 2014; accepted 8 February 2014; posted 10 February 2014 (Doc. ID 201308); published 18 March 2014

A novel approach is proposed to unwrap the phase maps of two fringe patterns in fringe pattern projection-based profilometry. In contrast to existing techniques, where spatial frequencies (i.e., the number of fringes on a pattern) of the two fringe patterns must be integers and coprime, the proposed method is applicable for any two fringe patterns with different fringe wavelengths (i.e., the number of pixels in a fringe) and thus provides more flexibility in the use of fringe patterns. Moreover, compared to the existing techniques, the proposed method is simpler in its implementation and has better antierror capability. Theoretical analysis and experiment results are presented to confirm the effectiveness of the proposed method.

OCIS codes: (120.5050) Phase measurement; (100.2650) Fringe analysis; (100.5088) Phase unwrapping.

http://dx.doi.org/10.1364/AO.53.001794

1. Introduction

With the development of digital technology, the noncontact three-dimensional (3D) shape measurement system using digital fringe projection (i.e., fringe projection profilometry [FPP]) has become an enabling technology for many applications [1–4]. Among various approaches, these based on the phase maps of the fringe patterns are the most commonly utilized. However, the phase maps acquired from the patterns are always wrapped into the range from $-\pi$ to π, leaving 2π jumps and drops in their values. In order to retrieve the surface shape, this type of discontinuity must be removed by the process known as phase unwrapping [5]. However, the phase unwrapping is usually a challenging task due to complex surfaces, noisy images, and ambient interferences [6], and hence various approaches have been developed [7,8]. The temporal phase unwrapping is a kind of method, which employ multiple fringe patterns with different frequencies. In order to keep the efficiency, it is always desirable to employ as few images as possible, and use of two images is the best selection. In [9,10], two fringe images were used, one of which has very low frequency to ensure its absolute phase value lying in $(-\pi, \pi)$. In [11,12], a projection image containing a single fringe was taken as a reference to

1559-128X/14/091794-08$15.00/0

simplify calculation. It has been noticed that if the gap between the frequencies of the two fringe patterns is larger than a certain value, the beforementioned methods would fail under noise and disturbance [13–17]. Hence some intermediate fringe patterns should be employed. In order to maintain the accuracy of phase unwrapping, and at the same time to keep the number of fringe patterns to a minimum, Ding *et al.* [18] proposed an approach to recover absolute phase maps of two fringe patterns with selected frequencies. A unique mapping was explored between the wrapped phase map and the fringe orders, and a lookup table was constructed to determine the absolute phase map.

While the method proposed in [18] provided an effective way to unwrap the two phase maps with selected frequencies, it also suffers from a limitation. As the two frequencies defined in [18] are the number of fringes on the images, these two frequencies, denoted by f_1 and f_2, are assumed to be integers, which are also required to be coprime as proved in [19]. In order to meet such a requirement, the total number of pixels perpendicular to the fringe must be an integer multiple of the number of pixels within a fringe. Such a selection may not be possible in some cases. Taking the experiment described in [18] as an example, the resolution of the projector is 1392×1038 pixels. If the selected frequencies are $f_1 = 8$ and $f_2 = 15$ as in [18], the numbers of pixels per fringe period will be 174 and 92.8, respectively, which are not integers and thus are not implementable. In fact, for the cases of the horizontal resolution being 1024 pixels, which is common for many ordinary projectors, it is impossible to find a pair of frequencies meeting the requirement of two frequencies being integers and coprime. A possible solution to this problem is to tailor the whole image to a smaller size, which may lead to the degradation of resolution in the 3D measurement.

In order to solve the above mentioned problem, we propose to employ a new way for designing the two fringe patterns. Instead of using the two frequencies f_1 and f_2, we choose the fringe waveform lengths λ_1 and λ_2 to describe the two fringe patterns, which are positive integers representing the total number of pixels in a fringe period. With the proposed method, the number of fringes on the projected image patterns does not need to be an integer, thus yielding more flexibility for the design of the patterns.

The paper is organized as follows. In Section 2 we first present the modified phase unwrapping method. In Section 3, the principle for fringe wavelength selection is analyzed. In Section 4, the phase error bound is given. In Section 5, experiments are presented to validate the proposed method. At last, Section 6 concludes the paper.

2. Modified Method

Consider that two sinusoidal fringe patterns are projected onto the surface of an object, which are reflected and captured by a camera. The two fringe patterns are with different wavelengths, denoted by λ_1 and λ_2, respectively, whose intensity varies in a sinusoidal manner vertically (i.e., in the y direction). Due to their sinusoidal nature, these fringe patterns can be described by the phase maps whose value monotonically increases over a range of $2\pi N$, where N is the number of fringes. For a pixel noted as y_c in the phase map of the image captured by the camera (denoted as the camera image), there must be a corresponding pixel noted as y_p on the phase map of the projected image. Such a corresponding relationship must be unique and can be expressed as follows:

$$\begin{cases} \Phi_{p1}(y_p) = \Phi_{c1}(y_c) \\ \Phi_{p2}(y_p) = \Phi_{c2}(y_c) \end{cases}, \tag{1}$$

where $\Phi_{pi}(y_p)$, $(i = 1, 2)$ is the phase of the projected image, and $\Phi_{ci}(y_c)$, $(i = 1, 2)$ is the phase of the camera image. Note that all these phases are absolute as they demonstrate a monotonic increase over y. If the vertical resolution of the projector is R, the phase of the projected fringe patterns can be expressed as follows:

$$\begin{cases} \Phi_{p1}(y_p) = (2\pi/\lambda_1)y_p \\ \Phi_{p2}(y_p) = (2\pi/\lambda_2)y_p \end{cases}, \qquad y_p \in [0, R). \tag{2}$$

However, only the wrapped phases $\phi_{c1}(y_c)$ and $\phi_{c2}(y_c)$ can be obtained by the phase-shifting profilometry (PSP) from the deformed fringe patterns captured by the camera, whose values are wrapped into the range $[-\pi, \pi]$. These wrapped phases are related to their corresponding absolute phases $\Phi_{c1}(y_c)$ and $\Phi_{c2}(y_c)$ by the following:

$$\begin{cases} \Phi_{c1}(y_c) = 2\pi m_1(y_c) + \phi_{c1}(y_c) \\ \Phi_{c2}(y_c) = 2\pi m_2(y_c) + \phi_{c2}(y_c) \end{cases}, \tag{3}$$

where $m_1(y_c)$ and $m_2(y_c)$ are integers. To meet the expressions of Eqs. (1) and (2) without loss of generality, the ranges of $\phi_{c1}(y_c)$ and $\phi_{c2}(y_c)$ are shifted by π, yielding the following:

$$0 < \phi_{c1}(y_c), \qquad \phi_{c2}(y_c) < 2\pi, \tag{4}$$

Combining Eqs. (1)–(3), we have

$$\begin{cases} (2\pi/\lambda_1)y_p = 2\pi m_1(y_c) + \phi_1(y_c) \\ (2\pi/\lambda_2)y_p = 2\pi m_2(y_c) + \phi_2(y_c) \end{cases}, \qquad y_p \in [0, R). \tag{5}$$

A useful relationship can be yielded by analyzing Eq. (5); that is:

$$\frac{\lambda_1\phi_1(y_c) - \lambda_2\phi_2(y_c)}{2\pi} = m_2(y_c)\lambda_2 - m_1(y_c)\lambda_1. \tag{6}$$

Note that the left hand side of Eq. (6) can be obtained by PSP, which must be an integer because the right side is an integer. If there is a one-to-one correspondence between the right side and the pair of integers

$m_1(y_c)$ and $m_2(y_c)$, Eq. (6) reveals a way to determine these two integers based on the value of the left-hand side. For simplicity of expression, the subscript c is dropped in the following content.

Combining Eqs. (4) and (6), we have

$$-\lambda_2 < [\lambda_1\phi_1(y) - \lambda_2\phi_2(y)]/2\pi < \lambda_1 \tag{7a}$$

that is,

$$-\lambda_2 < [m_2(y)\lambda_2 - m_1(y)\lambda_1] < \lambda_1. \tag{7b}$$

At the same time, from Eq. (5) and the expressions in (4), we have

$$0 \le m_1(y) < R/\lambda_1 \tag{8}$$

$$0 \le m_2(y) < R/\lambda_2. \tag{9}$$

With inequalities Eqs. (7)–(9) above, a unique mapping from $[\lambda_1\phi_1(y) - \lambda_2\phi_2(y)]/2\pi$ to a pair of $m_1(y)$ and $m_2(y)$ can be identified. In order to prove the effectiveness of such a method, let us consider an example where $\lambda_1 = 23$, $\lambda_2 = 47$, and $R = 768$. By varying $m_1(y)$ and $m_2(y)$ over the range defined by Eqs. (8) and (9), we are able to obtain $m_2(y)\lambda_2 - m_1(y)\lambda_1$. Then we check the value against the range given by Eq. (7), and those meeting the condition can be listed in Table 1.

From Eq. (5), the whole range of y_p (i.e., $[0, R)$) can be separated based on the value of $m_1(y)$ and $m_2(y)$ as follows:

$$m_1(y) = \begin{cases} 0, & 0 \le y_p < \lambda_1 \\ 1, & \lambda_1 \le y_p < 2\lambda_1 \\ \cdots & \cdots \\ [R/\lambda_1] - 1, & \lambda_1([R/\lambda_1] - 1) \le y_p < \lambda_1[R/\lambda_1] \\ [R/\lambda_1], & \lambda_1[R/\lambda_1] \le y_p < R \end{cases} \tag{10}$$

and

$$m_2(y) = \begin{cases} 0, & 0 \le y_p < \lambda_2 \\ 1, & \lambda_2 \le y_p < 2\lambda_2 \\ \cdots & \cdots \\ [R/\lambda_2] - 1, & \lambda_2([R/\lambda_2] - 1) \le y_p < \lambda_2[R/\lambda_2] \\ [R/\lambda_2], & \lambda_2[R/\lambda_2] \le y_p < R \end{cases}. \tag{11}$$

As the vertical resolution of the projection image is $R = 768$, from Eqs. (10) and (11) we can see that the first and second columns of Table 1 cover all the possible values of $m_1(y)$ and $m_2(y)$, and the third column meets the requirement of the desired range $-\lambda_2 < [m_2(y)\lambda_2 - m_1(y)\lambda_1] < \lambda_1$ without repetition.

Table 1. Relationship of $m_2(y)\lambda_2 - m_1(y)\lambda_1$ and $m_1(y)$, $m_2(y)$ when $\lambda_1 = 23$, $\lambda_2 = 47$

$m_1(y)$	$m_2(y)$	$m_2(y)\lambda_2 - m_1(y)\lambda_1$
2	0	−46
4	1	−45
6	2	−44
8	3	−43
10	4	−42
12	5	−41
14	6	−40
16	7	−39
18	8	−38
20	9	−37
22	10	−36
24	11	−35
26	12	−34
28	13	−33
30	14	−32
32	15	−31
1	0	−23
3	1	−22
5	2	−21
7	3	−20
9	4	−19
11	5	−18
13	6	−17
15	7	−16
17	8	−15
19	9	−14
21	10	−13
23	11	−12
25	12	−11
27	13	−10
29	14	−9
31	15	−8
33	16	−7
0	0	0
2	1	1
4	2	2
6	3	3
8	4	4
10	5	5
12	6	6
14	7	7
16	8	8
18	9	9
20	10	10
22	11	11
24	12	12
26	13	13
28	14	14
30	15	15
32	16	16

The above example shows that two phase maps with coprime wavelengths can be unwrapped. In fact, for a pair of fringe patterns with noncoprime wavelengths, phase unwrapping can also be done by the above-mentioned approach. Let us consider another example where $\lambda_1 = 52$ and $\lambda_2 = 100$, which are obviously not coprime. Similar relationships can be obtained in Table 2, which enable us to determine $m_1(y)$ and $m_2(y)$.

Table 2. Relationship of $m_2(y)\lambda_2 - m_1(y)\lambda_1$ and $m_1(y)$, $m_2(y)$ when $\lambda_1 = 52$, $\lambda_2 = 100$

$m_1(y)$	$m_2(y)$	$m_2(y)\lambda_2 - m_1(y)\lambda_1$
13	6	−76
11	5	−72
9	4	−68
7	3	−64
5	2	−60
3	1	−56
1	0	−52
14	7	−28
12	6	−24
10	5	−20
8	4	−16
6	3	−12
4	2	−8
2	1	−4
0	0	0
13	7	24
11	6	28
9	5	32
7	4	36
5	3	40
3	2	44
1	1	48

Through the above analysis the absolute phase can be retrieved from the wrapped phase maps of two fringe patterns with selected fringe wavelengths by the following steps:

1. Select two fringe wavelengths (λ_1, λ_2) using the criteria described in Section 3 to ensure the unique mapping from $m_2(y)\lambda_2 - m_1(y)\lambda_1$ to a pair of $m_1(y)$ and $m_2(y)$ and construct a lookup table like Table 1.
2. Project the two fringe patterns onto the object and obtain the unwrapped phase maps $\phi_1(y)$ and $\phi_2(y)$.
3. Calculate $[\lambda_1\phi_1(y) - \lambda_2\phi_2(y)]/2\pi$ and round it to the nearest integer. Find the row of the table constructed in step 1 whose value of $m_2(y)\lambda_2 - m_1(y)\lambda_1$ is closest to the integer. Keep the records of $m_1(y)$ and $m_2(y)$ in the same row.
4. Retrieve the absolute phase maps by Eq. (3) using $m_1(y)$ and $m_2(y)$ acquired in step 3.

Furthermore, the process of creating the table does not need to take $\Phi_0(y)$ as the reference for analyzing the interval distribution of the fringe orders like in [18], and hence does not need to do the interval partition at all. As the only task required is to check the simple inequalities (7), the computation associated with construction of the table is much less than that required in [18]. However, although the two parameters λ_1 and λ_2 do not need to be coprime, there must be a constraint to ensure the unique mapping from $m_2(y)\lambda_2 - m_1(y)\lambda_1$ to a pair of $m_1(y)$ and $m_2(y)$, which we will discussed in Section 3.

3. Selection of the Two Fringe Wavelengths

The validity of the above proposed method relies on the existence of unique mapping from $m_2(y)\lambda_2 - m_1(y)\lambda_1$ to a pair of $m_1(y)$ and $m_2(y)$. This requires that both sides of Eq. (6) must not yield the same value for any two different pixel number indices such as y_a and y_b $(a \neq b)$. In other words, the following must hold:

$$[\lambda_2 m_2(y_a) - \lambda_1 m_1(y_a)] \neq [\lambda_2 m_2(y_b) - \lambda_1 m_1(y_b)], \quad \text{for } y_a \neq y_b. \tag{12}$$

The above can be proved by reductio ad absurdum. Let us first discuss the simpler case where λ_1 and λ_2 are coprime. Without loss of generality, let us assume that $m_2(y) < \lambda_1$ and $m_1(y) < \lambda_2$ (that is, the number of fringes on one image is less than the number of pixels in a fringe of another image). Combining inequalities (8) and (9), we have $0 \leq m_1(y) < R/\lambda_1 \leq \lambda_2$ and $0 \leq m_2(y) < R/\lambda_2 \leq \lambda_1$; that is,

$$R \leq \lambda_1\lambda_2. \tag{13}$$

Then suppose there exist y_a and y_b $(a \neq b)$ making two side of (12) equal. There are three possible situations making the two pairs of $(m_1(y), m_2(y))$ different: $m_1(y_a) \neq m_1(y_b)$ and $m_2(y_a) \neq m_2(y_b)$; $m_1(y_a) \neq m_1(y_b)$ and $m_2(y_a) = m_2(y_b)$; $m_1(y_a) = m_1(y_b)$ and $m_2(y_a) \neq m_2(y_b)$. Without losing generality, we take the first case into account where $m_1(y_a) \neq m_1(y_b)$ and $m_2(y_a) \neq m_2(y_b)$. When the two sides of Eq. (12) are equal, we have:

$$[m_2(y_a) - m_2(y_b)]/\lambda_1 = [m_1(y_a) - m_1(y_b)]/\lambda_2, \quad \text{for } y_a \neq y_b. \tag{14}$$

As λ_1 and λ_2 are coprime, Eq. (14) must be equivalent to the following:

$$[m_2(y_a) - m_2(y_b)] = n\lambda_1 \quad \text{and} \quad [m_1(y_a) - m_1(y_b)] = n\lambda_2. \tag{15}$$

where n is an integer and $n \neq 0$. Combining Eqs. (8) and (9), we have $-R/\lambda_2 < [m_2(y_a) - m_2(y_b)] < R/\lambda_2$ and $-R/\lambda_1 < [m_1(y_a) - m_1(y_b)] < R/\lambda_1$, which means that $-R/\lambda_2 < n\lambda_1 < R/\lambda_2$ and $-R/\lambda_1 < n\lambda_2 < R/\lambda_1$. Considering the constraint given in Eq. (13), we have $-\lambda_1 \leq -R/\lambda_2 < n\lambda_1 < R/\lambda_2 \leq \lambda_1$ and $-\lambda_2 < n\lambda_2 < \lambda_2$. The result is $-1 < n < 1$(i.e., $n = 0$), which is in contradiction with $n \neq 0$. Hence, Eq. (14) will not be true when $R \leq \lambda_1\lambda_2$.

In the same way, we can prove that Eq. (12) holds for the other two cases.

Now we consider the case where λ_1 and λ_2 are not coprime. Letting k be the greatest common divisor (g.c.m.) of them, we have $\lambda_1 = kg_1$ and $\lambda_2 = kg_2$ where g_1 and g_2 are positive integers which are coprime. Equation (12) can be reproduced as follows:

$$[kg_2 m_2(y_a) - kg_1 m_1(y_a)] \neq [kg_2 m_2(y_b) - kg_1 m_1(y_b)], \quad \text{for } y_a \neq y_b \tag{16}$$

that is,

$$[g_2m_2(y_a) - g_1m_1(y_a)] \neq [g_2m_2(y_b) - g_1m_1(y_b)], \quad \text{for } y_a \neq y_b. \tag{17}$$

Obviously Eq. (17) is the same as Eq. (12), and hence can be proved using the same approach. Also Eq. (17) must hold when $R' \leq g_1g_2$, where $R' = R/k$, which is equivalent to $R \leq \lambda_1\lambda_2/k$. Therefore, we proved that, in the case where λ_1 and λ_2 are not coprime, Eq. (12) still holds when $R \leq \lambda_1\lambda_2/k$.

We can see from the above that there exists a unique mapping from $(m_1(y), m_2(y))$ to $[\lambda_1\phi_1(y) - \lambda_2\phi_2(y)]/2\pi$ [i.e., $m_2(y)\lambda_2 - m_1(y)\lambda_1$] when $R \leq \lambda_1\lambda_2/k$, where R is the resolution of projection and k is the g.c.m. of λ_1 and λ_2. Note that there is not any other restriction on the values of λ_1 and λ_2. In other words, the proposed approach provides more flexibility in the selection of the two wavelengths in contrast to the method presented in [18] and [19].

4. Phase Error Bound

The antierror capability of the proposed technique depends on the smallest gap between any two possible values of $[\lambda_1\phi_1(y) - \lambda_2\phi_2(y)]/2\pi$. The larger the gap, the less likely the error will happen during the rounding operation.

From Eq. (10), the range of y can be divided into $N_1 = [R/\lambda_1] + 1$ intervals in which the values of $m_1(y)$ are different, where $[x]$ denotes the largest integer not greater than x. The boundaries of the intervals are $n_1\lambda_1$ where $1 \leq n_1 < [R/\lambda_1]$. Similarly, from Eq. (11), the range of y can be divided into $N_2 = [R/\lambda_2] + 1$ intervals in which the values of $m_2(y)$ are different and the boundaries of the intervals are $n_2\lambda_2$ where $1 \leq n_2 < [R/\lambda_2]$.

Let us look at the case when λ_1 and λ_2 are coprime. It is obvious that $n_1\lambda_1 \neq n_2\lambda_2$, implying that the two types of boundaries will not coincide with each other. Hence, the two types of intervals of y shown above will not overlap. Combining Eqs. (10) and (11), y can be divided into N intervals, on which $\lambda_2m_2(y) - \lambda_1m_1(y)$ takes different values, and N is given by

$$N = N_1 + N_2 - 1 = [R/\lambda_1] + [R/\lambda_2] + 1. \tag{18}$$

From the range of $\lambda_2m_2(y) - \lambda_1m_1(y)$ given in Eq. (7), the average value gap is

$$G = \frac{\lambda_1 + \lambda_2 - 1}{[R/\lambda_1] + [R/\lambda_2] + 1}. \tag{19}$$

As $R \leq \lambda_1\lambda_2$, it is easy to show that $[R/\lambda_1] \leq R/\lambda_1 \leq \lambda_2$ and $[R/\lambda_2] \leq R/\lambda_2 \leq \lambda_1$, based on which we have $G = (\lambda_1 + \lambda_2 - 1)/([R/\lambda_1] + [R/\lambda_2] + 1) \geq 1$. Since, $\lambda_2m_2(y) - \lambda_1m_1(y)$ (i.e., $[\lambda_1\phi_1(y) - \lambda_2\phi_2(y)]/2\pi$) are positive integers, the gap of any two different possible values must be equal to or greater than 1. We can also shown that the minimal gap is 1 when $R = \lambda_1\lambda_2$. This particular case is the same as that in [19] where the normalized frequencies are $f_1 = R/\lambda_1 = \lambda_2$ and $f_2 = R/\lambda_2 = \lambda_1$.

Now considering the situation when λ_1 and λ_2 have the g.c.m. of k, we will see that the minimal gap must be equal to or greater than k as follows.

Let $\lambda_1 = kg_1$ and $\lambda_2 = kg_2$ where g_1 and g_2 are positive integers, which are coprime, we have $[\lambda_2m_2(y) - \lambda_1m_1(y)] = k\{[g_2m_2(y) - g_1m_1(y)]$. As proved above, the minimal gap among the different values of $g_2m_2(y) - g_1m_1(y)$ must be equal to or greater than 1, and hence the minimal gap of $\lambda_2m_2(y) - \lambda_1m_1(y)$ must be equal to or greater than k.

With the nominal gap determined above, we can look at the maximal error allowed in the wrapped phase maps, which will not result in an arborous phase unwrapping. Assuming phase errors in the phase maps $\phi_1(y)$ and $\phi_2(y)$ are $\Delta\phi_1(y)$ and $\Delta\phi_2(y)$, respectively, and $\Delta\phi_{\max} = \max(|\Delta\phi_1(y)|, |\Delta\phi_2(y)|)$, we have

$$\frac{[\lambda_1\Delta\phi_1(y) - \lambda_2\Delta\phi_2(y)]}{2\pi} < \frac{\lambda_1 + \lambda_2}{2\pi}\Delta\phi_{\max} < \frac{k}{2}. \tag{20}$$

Then the upper bounds of the allowable phase error with which the absolute phase maps can be correctly recovered are as follows:

$$0 \leq \Delta\phi_{\max} < \frac{k\pi}{\lambda_1 + \lambda_2}. \tag{21}$$

If $\Delta\phi_{\max}$ is given, the fringe wavelengths should be selected to meet the following:

$$\lambda_1 + \lambda_2 < \frac{k\pi}{\Delta\phi_{\max}}. \tag{22}$$

When λ_1 and λ_2 are coprime, $k = 1$, and the number of fringes on the images are integers, that is, $\lambda_1 = R/f_1$, $\lambda_2 = R/f_2$, Eq. (21) changes to

$$0 \leq \Delta\phi_{\max} < \frac{\pi}{\lambda_1 + \lambda_2} = \frac{\pi}{R/f_1 + R/f_2} = \frac{\pi}{R}\frac{f_1f_2}{f_1 + f_2}. \tag{23}$$

Since, $R \leq \lambda_1\lambda_2 = (R/f_1)(R/f_2)$, we have $f_1f_2 \leq R$; then Eq. (23) changes to

$$0 \leq \Delta\phi_{\max} < \frac{\pi}{R}\frac{f_1f_2}{f_1 + f_2} \leq \frac{\pi}{f_1 + f_2}. \tag{24}$$

The expression in Eq. (24) is the same as the conclusion in [19], implying that the method in [19] is a special case of the proposed approach. However the allowed range of phase error associated with the proposed method is larger than that in [19] when λ_1 and λ_2 are not coprime. For example, suppose the resolution of the projection image is $R = 120$, the selected frequencies are $f_1 = 8$ and $f_2 = 15$ (i.e., $\lambda_1 = 15$ and $\lambda_2 = 8$), which are described in [19] the upper bound of the allowable phase error is $0 \leq \Delta\phi_{\max} < \pi/23$. If

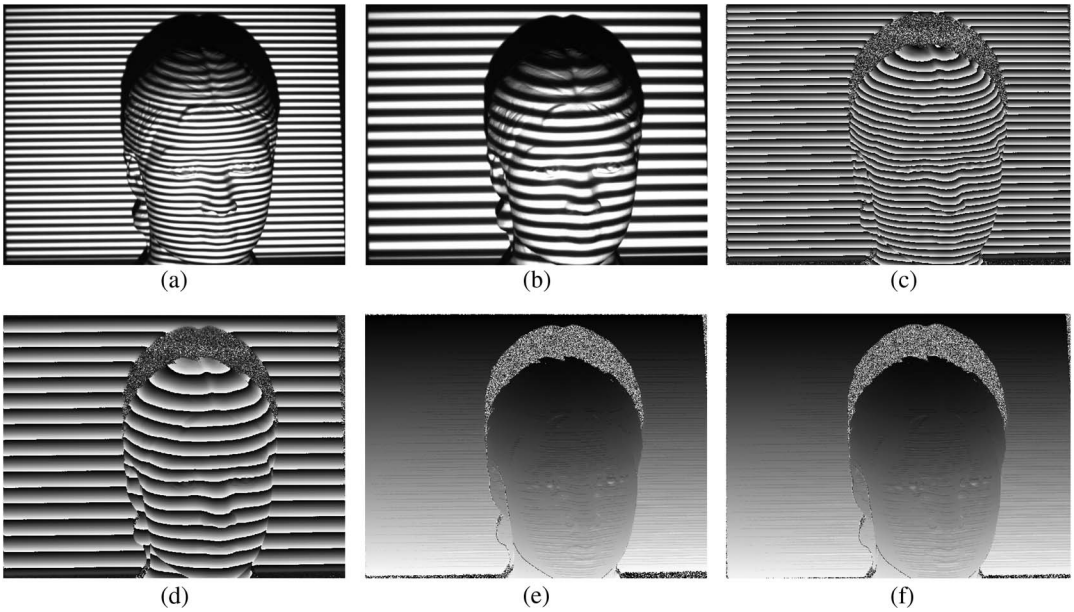

Fig. 1. Experiment results when $\lambda_1 = 23$, $\lambda_2 = 47$. (a) and (b) are the deformed fringe patterns, (c) and (d) are the wrapped phase maps, (e) and (f) are the recovered absolute phase maps of (c) and (d).

better antierror capability is needed, a pair of (λ_1, λ_2), which are not coprime can be selected, such as (34, 8). With such a selection, the upper bound for the phase error allowable expands to $0 \le \Delta\phi_{\max} < \pi/21$, implying that the proposed approach is more tolerant to phase errors. Also note that the method proposed in [19] cannot be used for such a selection of the two wavelengths.

5. Experiments

Experiments are carried out to test the proposed method where the resolution of the projector is 1024×768. First, two fringe patterns with fringe wavelengths of 23 and 47 are projected onto a plaster human head model, as shown in Figs. 1(a) and 1(b). The wrapped phase maps of them obtained from six-step PSP are shown in Figs. 1(c) and 1(d). The maximal phase error on the wrapped phase maps is about $\pi/100$, which is smaller than $k\pi/(\lambda_1 + \lambda_2) = \pi/70$. Hence, based on Eq. (21) the absolute phase maps can be successfully recovered. Figures 1(e) and 1(f) are the unwrapped phase maps, which are characterized by monotonic variance over the areas of smooth shape change on the face and reference plane, and hence results are considered as correct.

Second, two fringe patterns with fringe wavelengths 100 and 23 are projected onto a piece of paper. In order to show the results clearly, we captured part of the photo area. Because the width of the piece of paper is about half of the width of the projection

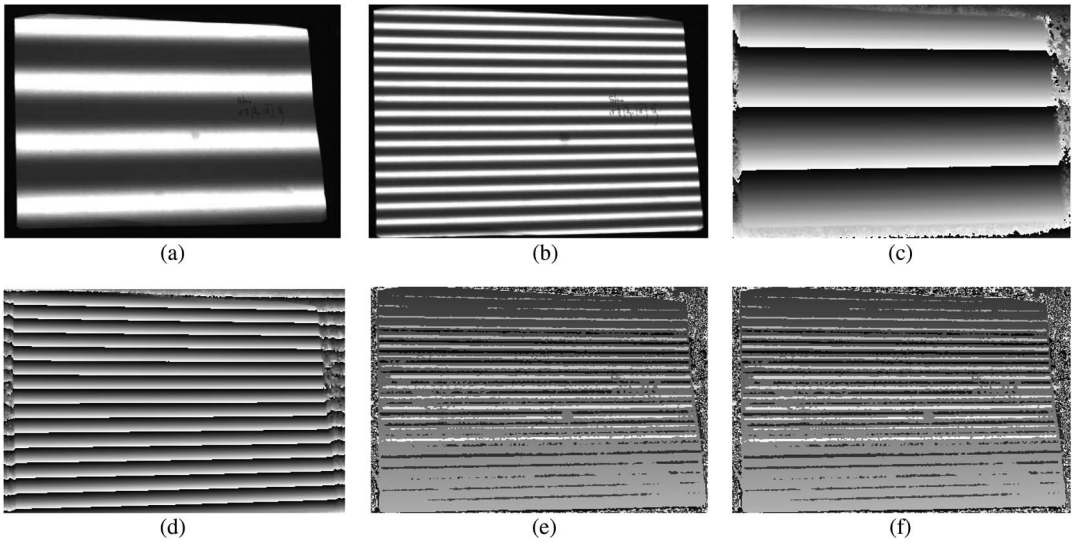

Fig. 2. Experiment results when $\lambda_1 = 100$, $\lambda_2 = 23$. (a) and (b) are the deformed fringe patterns, (c) and (d) are the wrapped phase maps, (e) and (f) are the recovered absolute phase maps of (c) and (d).

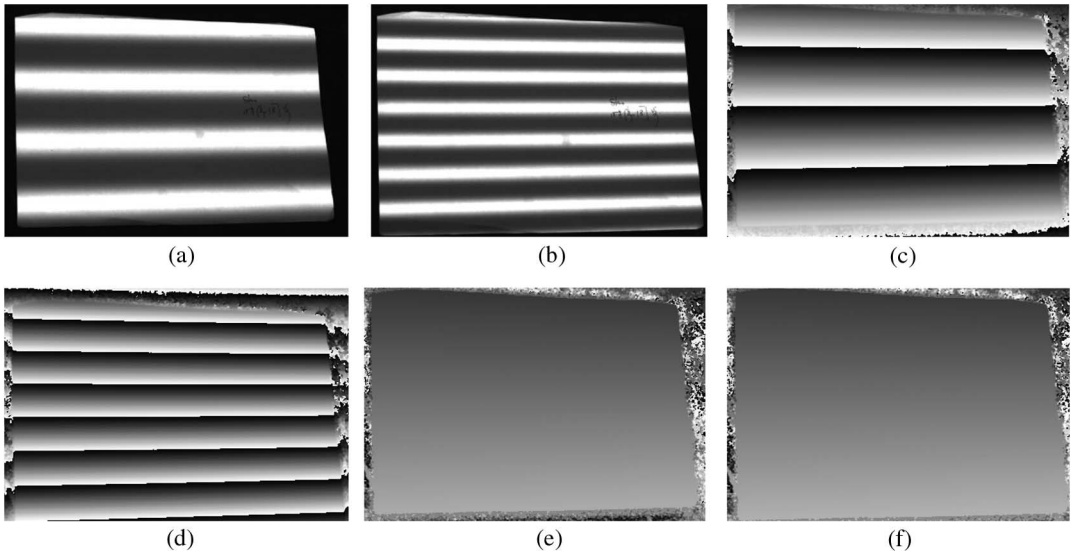

Fig. 3. Experiment results when $\lambda_1 = 100$, $\lambda_2 = 52$. (a) and (b) are the deformed fringe patterns, (c) and (d) are the wrapped phase maps, (e) and (f) are the recovered absolute phase maps of (c) and (d).

area, only about half number of the fringes can be seen on the paper. The two fringe patterns are shown in Figs. 2(a) and 2(b). The wrapped phase maps resulting from six-step PSP are shown in Figs. 2(c) and 2(d). Since, $k\pi/(\lambda_1 + \lambda_2) = \pi/123 < \pi/100$, according to the conclusion in Eq. (21), the proposed method may not be able to recover the absolute phase maps. Figures 2(e) and 2(f) are the results of unwrapped phase maps containing discontinuities and sharp changes, showing the occurrence of the phase unwrapping errors.

Third, two fringe patterns with wavelengths 100 and 52 are projected onto the same piece of paper, as shown in Figs. 3(a) and 3(b). The wrapped phase maps of them, which we get by six-step PSP are shown in Figs. 3(c) and 3(d).

Since, $k\pi/(\lambda_1 + \lambda_2) = \pi/38 > \pi/100$, according to the proposed method, the absolute phase maps can be recovered correctly, which are shown in Figs. 3(e) and 3(f).

6. Conclusion

A new method to unwrap the phase maps of two fringe patterns has been presented for FPP. Compared to existing work in [18] where the fringe patterns are described by spatial frequencies (i.e., the number of fringes in the pattern), the proposed method utilizes the fringe wavelength, leading to a number of advantages in contrast to the work in [18]. First, the method in [18] requires that the frequencies of the two fringe patterns be integers and coprime. In contrast, the proposed technique is applicable to any two fringe patterns of different fringe wavelengths (that is., the number of pixels within a fringe), thus providing more flexibility in the design of fringe patterns. Second, the proposed method is advantageous because less computation is required for constructing the checking tables than for the method in [18]. In additional, the proposed method is better than the one in [18] in terms of antierror capabilities. The effectiveness of the proposed method has been verified by experimental results.

References

1. P. S. Huang, C. Zhang, and F.-P. Chiang, "High-speed 3D shape measurement based on digital fringe projection," Opt. Eng. **42**, 163–168 (2003).
2. L. Kinell, "Spatiotemporal approach for real-time absolute shape measurements by use of projected fringes," Appl. Opt. **43**, 3018–3027 (2004).
3. J. Pan, P. S. Huang, and F.-P. Chiang, "Color phase-shifting technique for three-dimensional shape measurement," Opt. Eng. **45**, 013602 (2006).
4. S. Zhang and P. S. Huang, "High-resolution, real-time three-dimensional shape measurement," Opt. Eng. **45**, 123601 (2006).
5. S. Zhang, X. Li, and S. T. Yau, "Multilevel quality-guided phase unwrapping algorithm for real-time three-dimensional shape reconstruction," Appl. Opt. **46**, 50–57 (2007).
6. D. C. Ghiglia and M. D. Pritt, *Two-Dimensional Phase Unwrapping: Theory, Algorithms, and Software* (Wiley, 1998).
7. J. M. Huntley and H. O. Saldner, "Temporal phase-unwrapping algorithm for automated interferogram analysis," Appl. Opt. **32**, 3047–3052 (1993).
8. H. J. Chen, J. Zhang, D. J. Lv, and J. Fang, "3-D shape measurement by composite pattern projection and hybrid processing," Opt. Express **15**, 12318–12330 (2007).
9. H. Zhao, W. Chen, and Y. Tan, "Phase-unwrapping algorithm for the measurement of three-dimensional object shapes," Appl. Opt. **33**, 4497–4500 (1994).
10. J. Li, L. G. Hassebrook, and C. Guan, "Optimized two-frequency phase-measuring profilometry light-sensor temporal-noise sensitivity," J. Opt. Soc. Am. A **20**, 106–115 (2003).
11. J. L. Li, H. J. Su, and X. Y. Su, "Two-frequency grating used in phase-measuring profilometry," Appl. Opt. **36**, 277–280 (1997).
12. K. Liu, Y. Wang, D. L. Lau, Q. Hao, and L. G. Hassebrook, "Dual-frequency pattern scheme for high-speed 3-D shape measurement," Opt. Express **18**, 5229–5244 (2010).

13. J. M. Huntley and H. O. Saldner, "Error-reduction methods for shape measurement by temporal phase unwrapping," J. Opt. Soc. Am. A **14**, 3188–3196 (1997).
14. H. O. Saldner and J. M. Huntley, "Temporal phase unwrapping: application to surface profiling of discontinuous objects," Appl. Opt. **36**, 2770–2775 (1997).
15. S. Zhang, "Phase unwrapping error reduction framework for a multiple-wavelength phase-shifting algorithm," Opt. Eng. **48**, 105601 (2009).
16. S. Zhang, "Digital multiple wavelength phase shifting algorithm," Proc. SPIE **7432**, 74320N (2009).
17. C. E. Towers, D. P. Towers, and J. D. C. Jones, "Absolute fringe order calculation using optimised multifrequency selection in full-field profilometry," Opt. Lasers Eng. **43**, 788–800 (2005).
18. Y. Ding, J. Xi, Y. Yu, and J. Chicharo, "Recovering the absolute phase maps of two fringe patterns with selected frequencies," Opt. Lett. **36**, 2518–2520 (2011).
19. Y. Ding, J. Xi, Y. Yu, W. Q. Cheng, S. Wang, and J. Chicharo, "Frequency selection in absolute phase maps recovery with two frequency projection fringes," Opt. Express **20**, 13238–13251 (2012).